

Climatological phytoplankton chlorophyll and sea surface temperature patterns in continental shelf and slope waters off the northeast U.S. coast

James A. Yoder and Stephanie E. Schollaert

Graduate School of Oceanography, University of Rhode Island, Narragansett, Rhode Island 02882

John E. O'Reilly

Northeast Fisheries Center, Narragansett Laboratory, NOAA/NMFS, Narragansett, Rhode Island 02882

Abstract

Satellite-derived chlorophyll estimates from the Sea-viewing Wide Field-of-view Sensor (SeaWiFS) and Coastal Zone Color Scanner (CZCS), a large archive of in situ near-surface chlorophyll data, and satellite sea surface temperature (SST) measurements were used to quantify spatial and seasonal variability of near-surface chlorophyll and SST in middle shelf to slope waters off the coast of the U.S. Northeast. The results of empirical orthogonal function (EOF) analysis on normalized monthly fields (after temporal and spatial means were removed) show that all three chlorophyll climatologies have similar mode 1 temporal and spatial patterns in these waters. Mode 1, which explains about half of the total variability in monthly climatological images, shows that shelf waters in the Gulf of Maine (GOM) are out of phase with the mid-Atlantic bight (MAB), with seasonally high chlorophyll concentrations in winter in the MAB and in summer in the GOM. The three chlorophyll climatologies begin to differ at higher modes (modes 2 and 3), although SeaWiFS and in situ climatologies keep similar features through mode 3. Higher modes in both SST and chlorophyll are related to the effects of tidal mixing on Georges Bank, differences in seasonal stratification between the southwestern and northeastern GOM, and the importance of the spring bloom in MAB outer shelf waters and western GOM. SST patterns during the CZCS and SeaWiFS eras are very similar, and this indicates that the observed differences between results obtained with these two sensors are probably not caused by differences in physical processes during the two satellite eras.

The shelf and slope waters off the coast of the U.S. Northeast are some of the most productive in the world (Ryther and Yentsch 1958; O'Reilly et al. 1987; Csanady 1990). Our study focuses on continental shelf and slope waters, an area where depths range between 20 and 500 m, including the mid-Atlantic bight (MAB), Georges Bank (GB), and the Gulf of Maine (GOM) (Fig. 1). Previous results based on Coastal Zone Color Scanner (CZCS) imagery binned in time and space show that the MAB has a simple annual cycle in chlorophyll concentration consisting of a broad peak during winter and minimum concentrations during summer (Yoder et al. 2001). In situ observations confirm that the northern GOM waters have seasonal peak chlorophyll concentrations in March and April (Townsend and Spinrad 1986; O'Reilly and Zetlin 1998) and a secondary spring peak is also observed in outer shelf and slope waters of the MAB (Brown et al. 1985; Yoder et al. 2001). In situ and CZCS data also show high variability at time scales of days to weeks associated with wind forcing and other processes (Walsh et al.

1978, 1987; Eslinger et al. 1989; Flagg et al. 1994; Yoder et al. 2001). For example, Gulf Stream rings influence phytoplankton distribution patterns in slope waters (Ryan et al. 2001), and mixing associated with frontal dynamics leads to enhanced phytoplankton biomass concentrations and productivity in the shelf-slope frontal region compared to adjacent waters (Marra et al. 1990; Ryan et al. 1999).

Understanding the spatial and temporal patterns of the near-surface chlorophyll concentrations in this region, as well as the consistency between ocean color satellite (CSAT) data sets, is the motivation for our study. We analyzed multiyear averages of monthly chlorophyll composites derived from CZCS, Sea-viewing Wide Field-of-view Sensor (SeaWiFS), and in situ data to determine if the three data sets show consistent spatial and temporal patterns. We also examined the corresponding spatial and temporal variability in satellite-derived sea surface temperature (SST) to ascertain any changes in physical forcing between the two satellite eras. The monthly climatologies we compare in this study consist of three chlorophyll *a* (Chl *a*) data sets—CZCS (1978–1986), SeaWiFS (Sept 1997–Aug 2000), and in situ (1977–1988) (Fig. 2)—as well as the corresponding SST (SeaWiFS era shown in Fig. 3). We used the empirical orthogonal function (EOF) method to separate the data into spatial functions and time-varying amplitudes to quantify the variability of the spatial patterns and address the following questions. At what spatial and temporal scales are the SeaWiFS and CZCS CSAT Chl *a* measurements comparable? Can the differences be explained by any change in the climatology using the SST data as an index of change between the CZCS and SeaWiFS eras? What physical forcing mechanisms explain the observed patterns?

Acknowledgments

We thank the SeaWiFS Project Office and NASA Goddard Distributed Active Archive Center (DAAC) for providing the high-resolution level 1a SeaWiFS data. Margarita Conkright, Dave Phinney, Charlie Yentsch, Charlie Flagg, and Barnie Balch are gratefully acknowledged for providing in situ surface chlorophyll data. We thank Dan Holloway, Dave Ullman, Sheekela Baker, and Carl Wolfteich for providing the AVHRR SST data and declouding codes. Additionally, this study benefited from discussions with Mete Uz, Dave Ullman, Maureen Kennelly, and Teresa Ducas and from the reviewers' comments. This work was funded by NASA HQ, NOAA, and the University of Rhode Island.

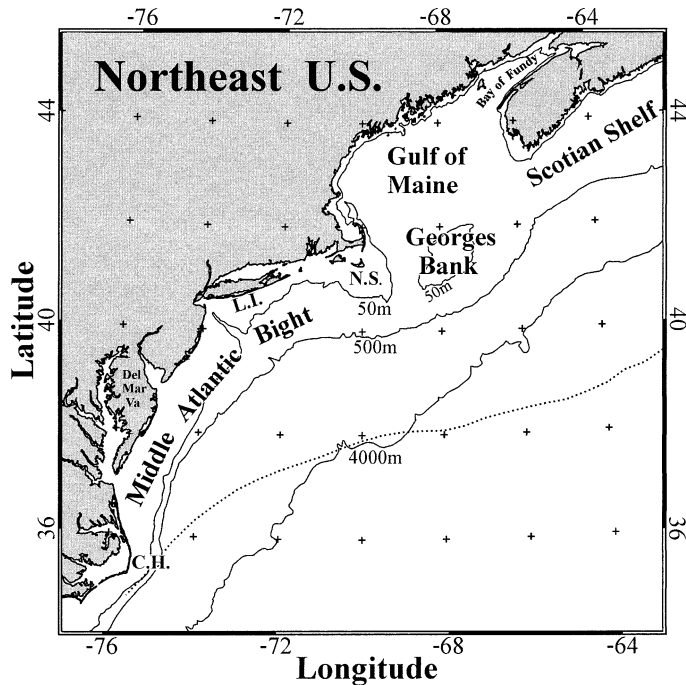


Fig. 1. Northeast United States study area and its major continental shelf regions: mid-Atlantic Bight, Georges Bank, Gulf of Maine, and Scotian shelf. Also shown for reference are Cape Hatteras (C.H.), the Delaware/Maryland/Virginia peninsula (Del-MarVa), Long Island (L.I.), Nantucket Shoals (N.S.), and Bay of Fundy. The 50-, 500-, and 4000-m bathymetry contours are delineated. An 18-yr average northern extent of the Gulf Stream is illustrated as a dashed line.

Materials and methods

High-resolution level 1 CZCS and SeaWiFS ocean color radiances were atmospherically corrected and processed to level 2 using SeaDAS version 4.0 (Baith et al. 2001). SeaDAS was also used to remap level 2 normalized water-leaving radiance (nLw) and Chl *a* estimates to our standard northeast coast (NEC) projection (Fig. 1). SeaWiFS Chl *a* was derived by NASA Version 3 processing using OC4v4 (McClain et al. 2000; O'Reilly et al. 2000) within SeaDAS with solar zenith threshold lowered to 70° and the following flags added to the mask: low nLw 555, solar zenith angle, straylight. In situ surface chlorophyll data were acquired and collated from many different sources, but most are from the National Oceanic and Atmospheric Administration (NOAA)–National Marine Fisheries Service (NMFS) multiyear study of the northeastern U.S. ecosystem, known as Marine Resource Monitoring and Prediction (MARMAP). MARMAP investigators made in situ chlorophyll measurements (>57,000 observations) during 78 oceanographic cruises between 1977 and 1988 (O'Reilly and Zetlin 1998), which overlaps the CZCS observation period. Methodology for chlorophyll measurements is described in detail elsewhere (O'Reilly and Zetlin 1998). In brief, water samples were filtered using Whatman GF/F filters, pigments were extracted using 90% acetone, and Chl *a* concentration was determined fluorometrically using standard methods

(Yentsch and Menzel 1963; Holm-Hansen et al. 1965). Monthly climatologies of in situ surface Chl *a* were made by placing all available data for a given month on a grid using a standard interpolation (weighting) scheme based on the distance between sample location and grid points. The resultant grids were then mapped to the same projection as the satellite data. The CZCS Chl *a* was calculated using the OC3g algorithm (O'Reilly et al. 1998) tuned with the same in situ data used in this study. We calculated monthly climatological chlorophyll concentrations for each data set by taking the geometric mean, or median, of all nonmissing and nonmasked values at each pixel. We chose to use the geometric rather than the arithmetic mean because the distribution of chlorophyll measurements in continental shelf and slope waters is approximated by a log-normal distribution (Campbell 1995; Yoder et al. 2001). Standard monthly global maps produced by the SeaWiFS Project use the arithmetic mean. In a previous study (Yoder et al. 2001), we compared results using different binning strategies for CZCS data. At typical high chlorophyll concentrations of shelf and slope waters, using either the geometric or arithmetic mean to bin data yielded very comparable monthly maps. The geometric mean has the additional advantage, however, of reducing the effect of a single high value on the mean. Such high values (outliers) may be more common in the full-resolution imagery that we used in our study than in the reduced spatial resolution global imagery used by the SeaWiFS Project (which has been smoothed to some extent by subsampling of the raw data). We excluded waters shallower than 20 m to avoid erroneous CSAT estimates resulting from CZCS sensor saturation over adjacent land (Evans and Gordon 1994) and bio-optically complex waters that confound simple empirical algorithms. We previously showed good agreement between in situ and CZCS chlorophyll concentrations for waters deeper than 20 m in our study area, particularly when considering broad spatial patterns and seasonal time scales (Yoder et al. 2001). For the past two decades, SST has been measured continuously by the Advanced Very High Resolution Radiometer (AVHRR) onboard a succession of NOAA polar-orbiting satellites. Here, we use SST derived from NOAA-14 (1997–2000) during the SeaWiFS era and Pathfinder-processed SST from NOAA-11 (1985–1987) to represent the CZCS era. In addition, after declouding the SST scenes (Cayula and Cornillon 1992), we calculated monthly SST climatologies for the CZCS and SeaWiFS eras by taking the median of each pixel.

EOF analysis is a useful technique for compressing the spatial and temporal variability of time series data down to the most energetic statistical modes. This method of data reduction was first applied to geophysical data by Lorenz (1956) for the purpose of statistical weather prediction. While the statistical EOF modes do not necessarily correspond to direct physical forcing mechanisms, partitioning the spatial and temporal variance of a data set into modes reveals spatial functions having time-varying amplitudes that can be interpreted in relation to physical processes. The time domain EOF analysis performed in this study will not detect propagating features (Emery and Thomson 1998). Here we apply the computationally efficient singular value decomposition (SVD) method to calculate eigenvectors, eigenval-

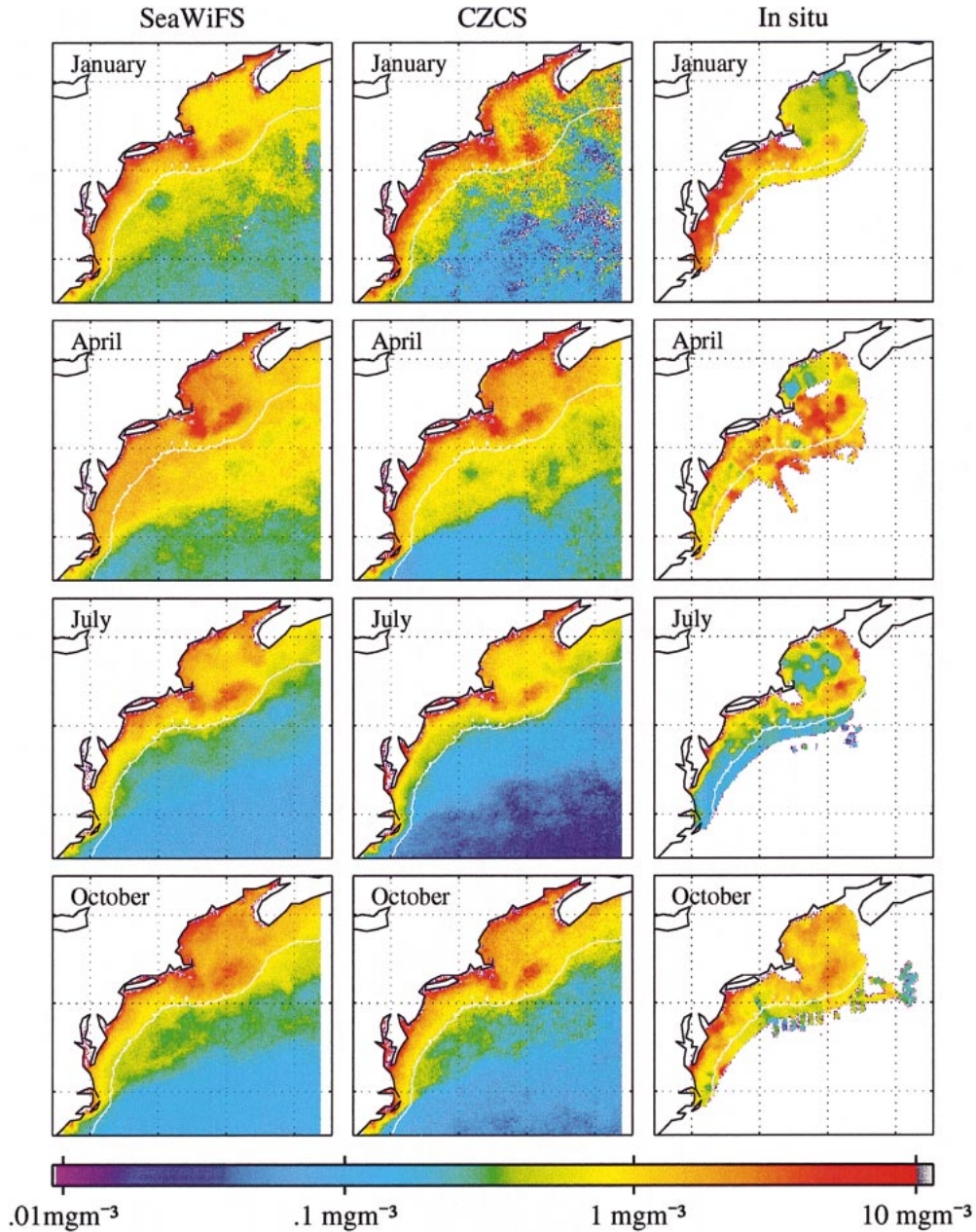


Fig. 2. Northeast Coast (NEC) chlorophyll concentrations from SeaWiFS, CZCS, and in situ climatological monthly composites for January (typifies winter), April (spring), July (summer), and October (fall). White contour delineates 500-m bathymetry.

ues, and time-varying amplitudes. Using SVD to determine EOFs yields identical results to the “brute force” covariance matrix method, with the decided advantage of not requiring the extensive computing resources to calculate the covariance matrix (Kelly 1988). Considering N monthly composites, the spatial and temporal variance of the data set, $x_m(t)$, can be partitioned into modes, i , revealing spatial functions, $\phi_i(m)$, having time-varying amplitudes, $a_i(t)$, also known as principle components, such that

$$x_m(t) = \sum_{i=1}^N [a_i(t)\phi_i(m)]$$

which means the time variation of the scalar data (chlorophyll or temperature) for each pixel is the summation of the spatial functions, ϕ_i , whose amplitudes, $a_i(t)$, indicate how the spatial modes vary with time. Eigenvalues can be considered as the portion of total variance explained by the EOF, where the sum of the variances in the data equals the sum of variance in the eigenvalues.

$$\sum_{m=1}^M \left\{ \frac{1}{N} \sum_{n=1}^N [x_m(t_n)]^2 \right\} = \sum_{j=1}^M \lambda_j$$

EOF analysis requires complete matrices and cannot skip

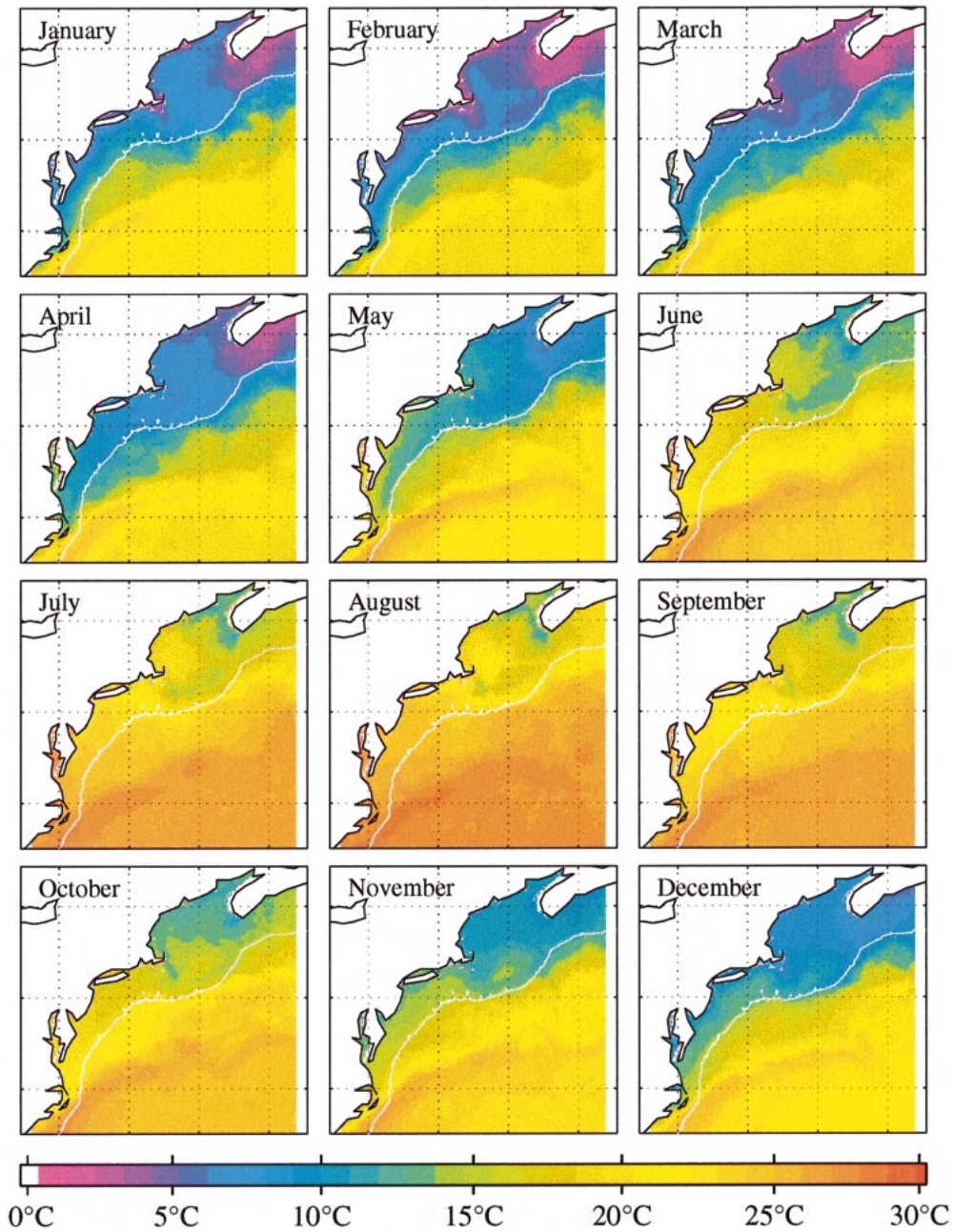


Fig. 3. Northeast Coast (NEC) AVHRR sea surface temperature climatological monthly composites (generated with September 1997–August 2000 data, a.k.a. SeaWiFS era). White contour delineates 500-m bathymetry.

over any missing data values. Prior to performing EOF analysis, any gaps in the data can be filled in or the gaps can be excluded from EOF calculations. In this study, we ran a three by three pixel median filter over the data to replace missing values over small gaps. Large gaps were not filled. Notably within the in situ data, there is a large gap northwest of Georges Bank in the February composite and a large gap in the central Gulf of Maine in April; these gaps resulted in the exclusion of those two areas for the EOF analyses. Monthly mean chlorophyll concentrations were converted to grey scale values according to the formula grey scale = $[\log(\text{chl}$

+ 2)] × 66.67. Grey scale values were used in all linear calculations performed in this study as appropriate for data that are log-normally distributed (Campbell 1995).

Because the sample size is so large in our study ($O \sim 10^5$), the uncertainty of the eigenvalues is insignificant ($O \sim 10^{-1}$) by the following relationship.

sampling error of an eigenvalue

$$\sim \lambda \left(\frac{2}{N} \right)^{1/2} \quad (\text{North et al. 1982})$$

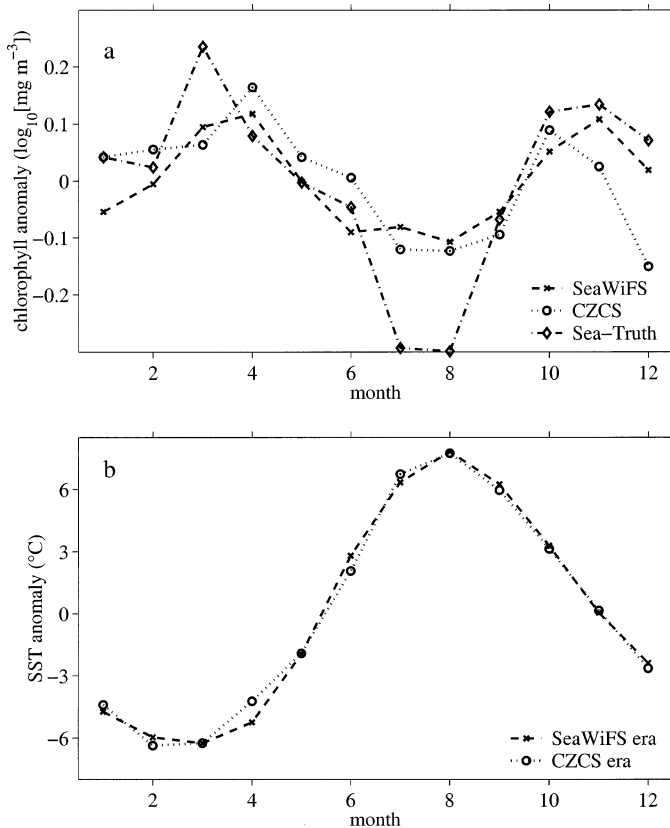


Fig. 4. Monthly spatial means after the removal of the temporal mean for (a) the three chlorophyll data sets and (b) SST during the SeaWiFS and CZCS eras. The chlorophyll anomaly is shown in \log_{10} units; therefore, the values (-0.1 , 0 , 0.1 , etc.) should be considered a ratio (e.g., 0 anomaly means the spatial mean is equal to the temporal mean; 0.1 anomaly is $\sim 25\%$ greater than the temporal mean; -0.1 is $\sim 20\%$ less).

For all chlorophyll and SST data sets, more than 98% of the variability is contained in the seasonal signal, so the first mode overwhelms the lesser modes. By removing the temporal and spatial means, the dominant seasonal signal was reduced. We also normalized by dividing each de-meant pixel by its standard deviation (Davis 1973). This procedure reduces the extremes in areas of high variability relative to areas of low variability without completely damping out the anomalies. Normalizing also nondimensionalizes the data, enabling us to calculate combined EOFs on coincident chlorophyll and temperature. One characteristic and advantage of a combined EOF is that the two variables (SST and chlorophyll in our case) will have the same principal components (time-varying amplitudes), thus making it very easy to detect and interpret common temporal (e.g., seasonal) patterns (Bretherton et al. 1992). Alternatively, if the two data sets are unrelated, the principal components will likely show random temporal fluctuations. It is also hypothetically possible that one of the two nondimensionalized data sets could dominate the resultant mode, in which case the other would have spatial function values approaching zero. Such a result would also indicate that the two data sets are independent of each other and share no common forcing mechanism.

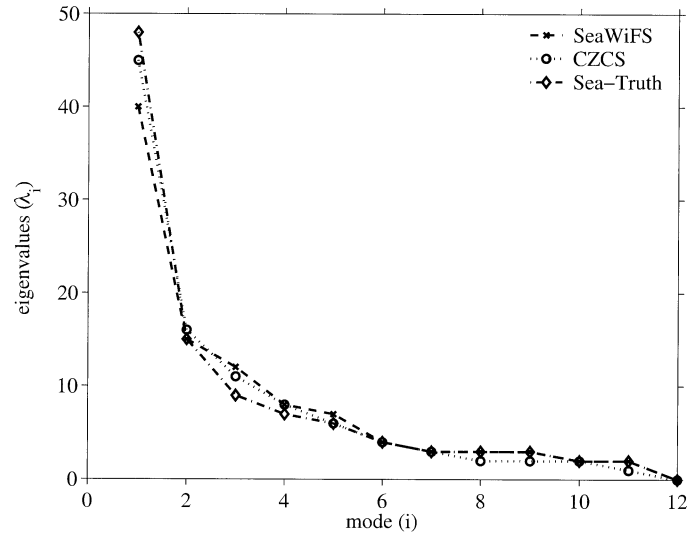


Fig. 5. Eigenvalues (λ_i) for SeaWiFS, CZCS, and in situ data. Mode 1 explains 40, 45, and 48% of the variability, respectively; mode 2, 15, 16, and 15%, respectively; mode 3, 12, 11, and 9%, respectively, and so on. Because the sample sizes are so large (SeaWiFS, 169,275 data points; CZCS, 169,225 data points; in situ, 108,690 data points), the uncertainty on the eigenvalues is insignificant ($O \sim 10^{-1}$).

Thus, we used the combined EOF technique to determine how closely the temporal and spatial SST and CSAT patterns are related. Prior to calculating combined EOFs, we merged the nondimensionalized pair of CSAT and SST fields for each month. For the SeaWiFS era, each matrix of the pair was 169,253 pixels by 12 months (see Figs. 2, 3); thus, the resultant merged matrix was 338,506 pixels by 12 months. For each monthly SST and chlorophyll image pair, we only used pixels for the merged matrix containing valid data in both of the two data sets. To help visualize the EOF results, the spatial function matrices were separated, after the EOF analyses, into chlorophyll and SST contributions for each mode; both are associated with a common eigenvalue and time-varying amplitude (principal component).

Results and discussion

Distribution of chlorophyll—The distribution of chlorophyll and SST throughout the study area during January, April, July, and October is illustrated in Figs. 2 and 3, respectively. EOF calculations using monthly mean chlorophyll that has not been de-meant or normalized yield one dominant mode, in which nearly all of the variability is explained by the seasonal cycle: 99.2% for CZCS; 99.7% for SeaWiFS; 98.0% for in situ. The spatial functions are nearly homogeneous (i.e., the whole region has the same sign and very nearly the same amplitude), and the time-varying amplitudes are dominated by broad seasonal peaks during winter–spring and again in the fall. Lowest chlorophyll concentrations in all three data sets occur in July/August. This seasonal signal can be considered mode 0. Previous studies detailed these phenomena, as well as their vertical characteristics, for this region (Fuentes-Yaco et al. 1997; Longhurst 1998; O’Reilly

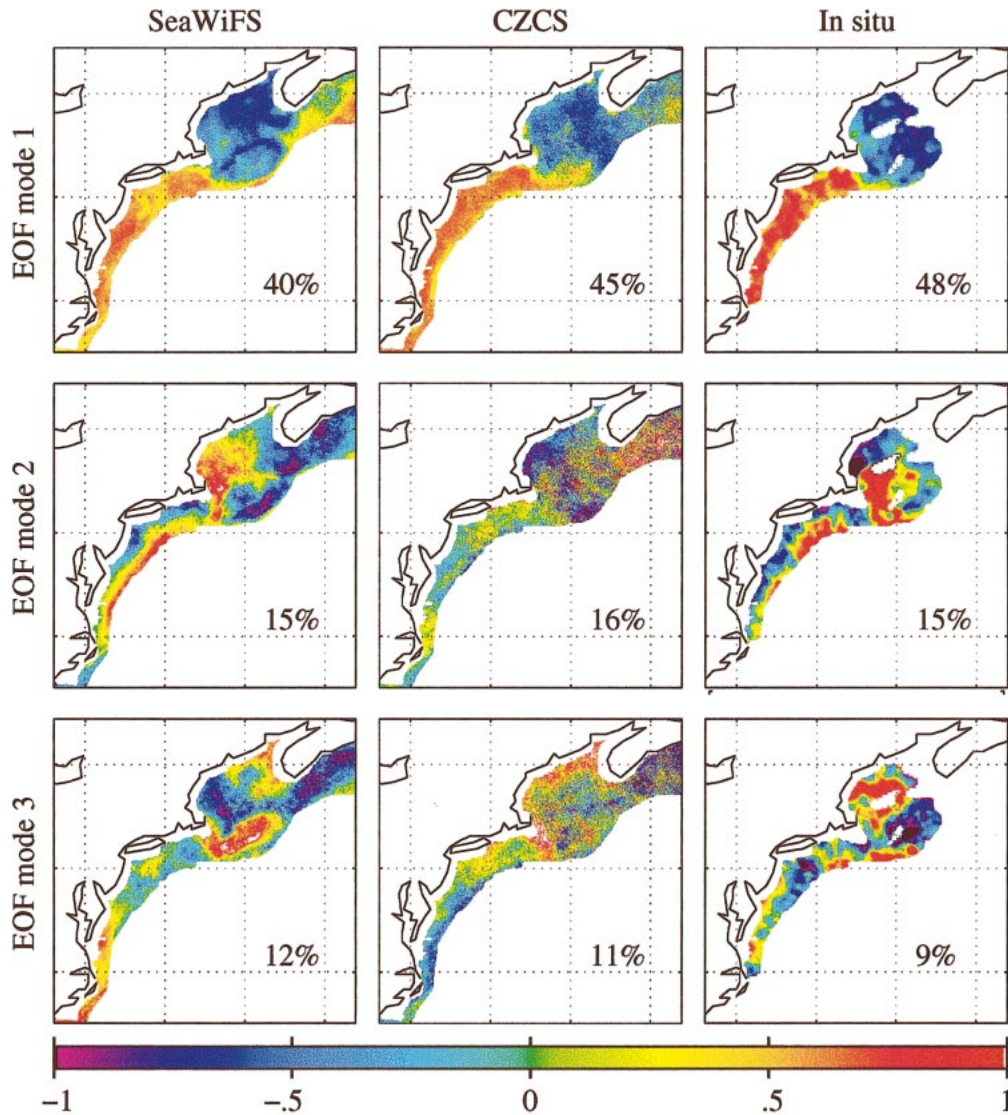


Fig. 6. Spatial eigenfunctions for SeaWiFS, CZCS, and in situ modes 1, 2, 3. Units are dimensionless and scaled for clarity.

and Zetlin 1998; Yoder et al. 2001). The temporal means show some areas of high mean chlorophyll (e.g., Georges Bank), but most MAB and GOM waters have similar mean values. After removing the temporal mean from each pixel, the monthly spatial means show a spring (Mar–Apr) and fall–winter (Oct–Dec) peak, with mean winter (Jan–Feb) concentrations higher than mean summer (Jun–Aug) concentrations (Fig. 4a). In our analyses, the terms “spatial mean” refers to the monthly average of all pixels once the temporal mean for each pixel has been subtracted. For example, positive values for the monthly spatial mean indicate months when chlorophyll was high compared to the temporal mean throughout the entire study area. Note that the spatial means of the in situ data are lower during July and August than for the two satellite data sets. The reason is evident from Fig. 2 because neither the empirical SeaWiFS nor CZCS algorithms capture the low (compared to in situ)

summer values in the western GOM or the southern portion of the MAB. SST spatial means for the SeaWiFS and CZCS periods are coherent with minima in March and maxima in August, reflecting the annual cycle of stratification of these waters (Fig. 4b). The rest of our analyses focus on the spatial and temporal variations relative to the results of Fig. 4.

After de-meaning and normalizing, EOF analyses on the resultant imagery show that the first four eigenvalues contain more than 75% of the variability of the spatial patterns, with the first mode explaining between 40 and 48% of the variability for all three chlorophyll data sets (Fig. 5). EOFs on data pretreated in this manner emphasize temporal changes to the general mean spatial pattern (i.e., when one or more of the study areas [pixels] change disproportionately more [or less] with time than the others). The pretreatment removes any common seasonal pattern so that the resultant amplitude time series show phase shifts associated with dif-

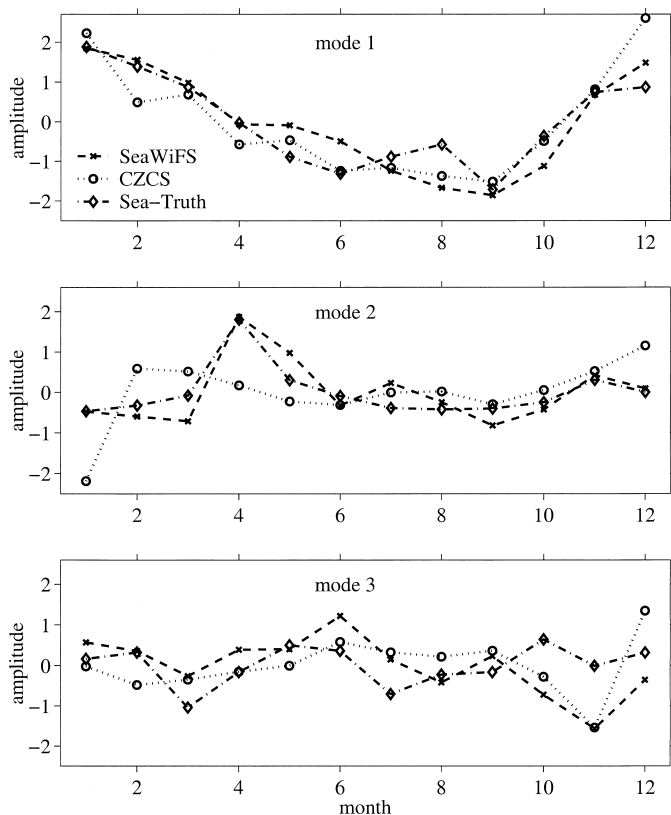


Fig. 7. Time-varying amplitudes for SeaWiFS, CZCS, and in situ modes 1, 2, 3. Units are dimensionless and scaled for clarity.

ferent spatial regions. EOFs from normalized data will show little or no effects if all temporal changes are in phase and in proportion to the initial spatial gradients.

The mode 1 spatial functions (Fig. 6) show high relative contrast between the MAB and GOM. In conjunction with the time-varying amplitude coefficients (Fig. 7), all three mode 1 EOFs indicate MAB shelf waters have the opposite sign from the GOM; thus, the MAB and GOM are out of phase by 6–8 months. MAB chlorophyll concentrations are highest during the winter, peaking in December/January, and lowest between April and October. By contrast, in the GOM, chlorophyll concentrations are low throughout the winter (between November and March) and high between April and October, peaking in August (SeaWiFS) and September (CZCS and in situ). The consistency between sensors, with only slight variations in the spatial functions and amplitude coefficients, implies that the signal is biological rather than a sensor or algorithm artifact.

Mode 2 explains 15% of the variability in the SeaWiFS and in situ data and 16% of the variability in the CZCS data. In this mode, however, CZCS data show more noise (e.g., pixel-to-pixel sign changes) and begin to diverge from the other two data sets spatially and temporally. This divergence is especially apparent in the amplitudes (Fig. 7) for the months with the sparsest data (December, January, February) and in the spatial functions over the Scotian shelf (Fig. 6). Divergence of the CZCS data from the other two data sets is also related to differences in the spatial means (Fig. 4),

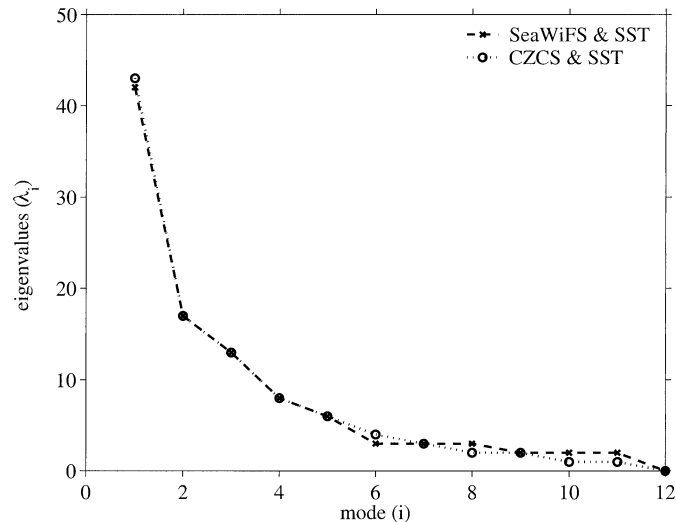


Fig. 8. Eigenvalues (λ_i) for SeaWiFS/SST and CZCS/SST. Mode 1 explains 42 and 43% of the variability, respectively; mode 2, 16 and 17%, respectively; mode 3, 12 and 13%, respectively; and so on. Again, the sample sizes are large (SeaWiFS/SST, 169,253 data points; CZCS/SST, 168,234 data points), so the uncertainty on the eigenvalues is insignificant ($O \sim 10^{-1}$).

which are subtracted prior to the analyses and thus affect the relative spatial patterns. Note that in Fig. 4, CZCS is very different from the other two data sets during October–December, and this difference contributes to the differences in the principal components and spatial patterns for those 3 months. The results from the EOF analyses are thus somewhat different from the visual impression one gets when looking at the monthly images (e.g., Fig. 2). Note that only pixels in waters shallower than 500 m were used for the EOF analyses; thus, the satellite data illustrated by the large offshore expanse of low-chlorophyll waters (blue colors) in Fig. 2 were not included in the EOF analyses. In the SeaWiFS and in situ data, the mode 2 spatial functions show that the outer shelf and western GOM have a different pattern than the middle shelf (20- to 60-m isobaths), Georges Bank, and Scotian shelf. The amplitude coefficients for SeaWiFS and in situ data indicate that chlorophyll concentrations on the outer shelf of the MAB and the western GOM experience their maximum peak in April, with a minor peak in November, but have relatively slightly lower concentrations than the middle shelf/Georges Bank/Scotian shelf during the rest of the year. These results indicate that the spring bloom and, to a lesser extent, the fall bloom bring the greatest relative increase in chlorophyll concentrations to the outer shelf of the MAB and western GOM. Thus, the spring and fall blooms cause less relative increase in MAB middle shelf waters, as is also evident in the monthly composites (Fig. 2).

By mode 3, SeaWiFS and in situ data also diverge from each other, possibly owing to the absence of in situ data for many of the areas from which the SeaWiFS spatial function was derived (i.e., Scotian shelf, Bay of Fundy outflow, vicinity of Cape Hatteras). CZCS continues to display more noise: the greatest deviations from the other two data sets occur spatially in the GOM and Georges Bank (Fig. 6) and

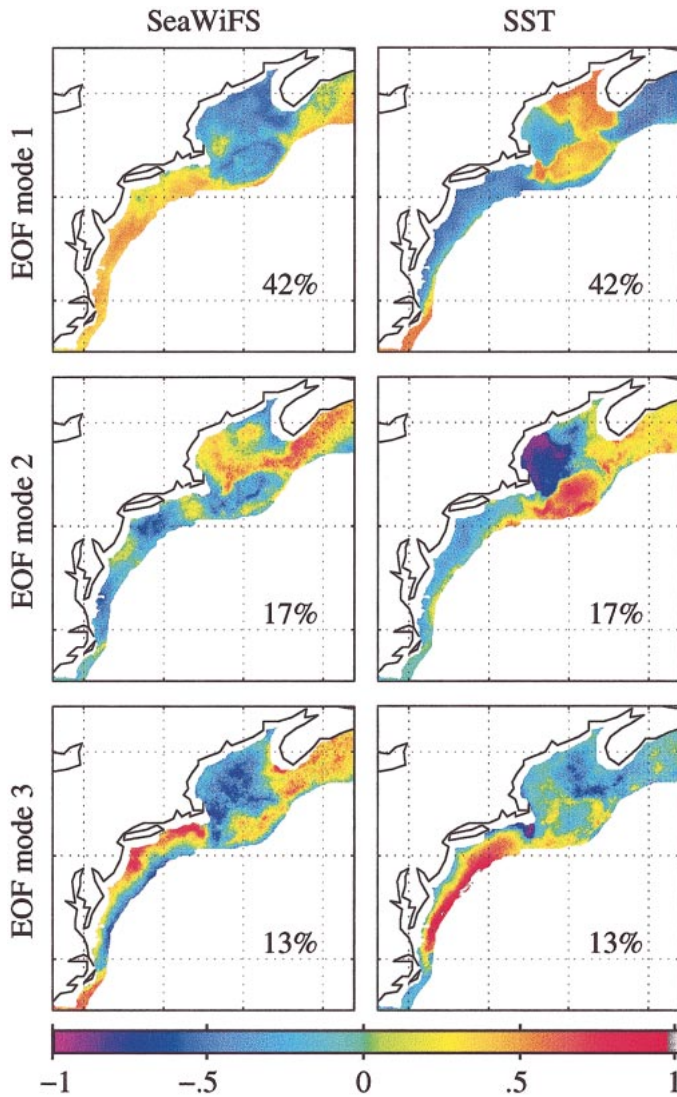


Fig. 9. Spatial eigenfunctions for SeaWiFS and SST combined EOF modes 1, 2, 3. Units are dimensionless and scaled for clarity.

temporally during winter (Fig. 7). The SeaWiFS EOFs indicate that the Bay of Fundy outflow, Georges Bank, Nantucket Shoals, a small area south of Long Island, and Cape Hatteras/DelMarVa all experience a relative chlorophyll peak in June and a low in November. The common feature of all these areas is that they are relatively shallow. The physical forcing mechanism related to this mode is likely tidal mixing, which supplies nutrients to these areas (e.g., Georges Bank) in May–June when deeper areas are nutrient limited (Bisagni and Sano 1993; Ullman and Cornillon 1999). By October–November, however, convective overturning experienced by the deeper areas outweighs tidal mixing as a source of nutrients.

*Distribution of chlorophyll combined with temperature—*Calculating EOFs on combined CSAT/SST pairs results in common eigenvalues (Fig. 8) and time-varying amplitudes (Figs. 10, 12) per mode and two independent spatial functions (Figs. 9, 11). Throughout most of the region, the spatial

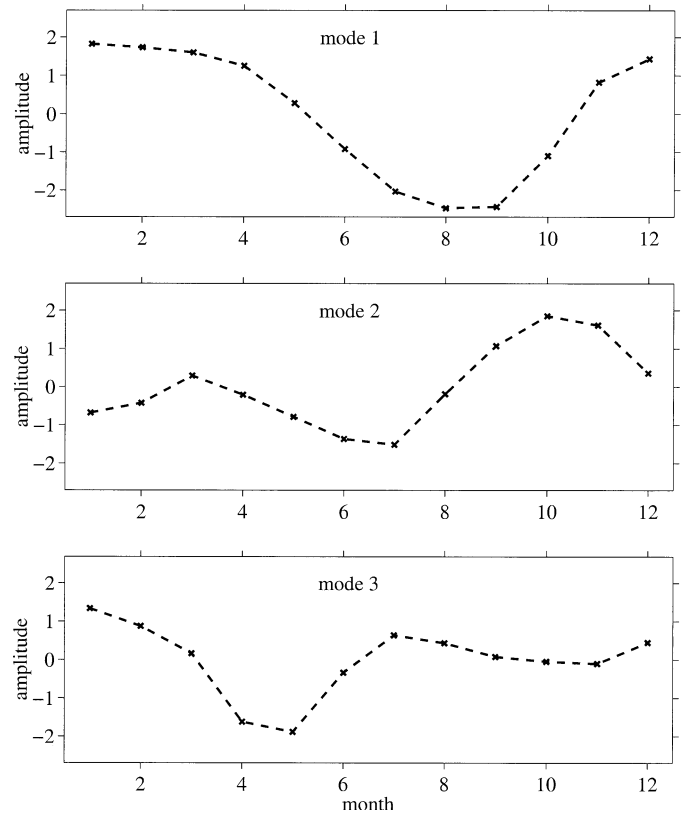


Fig. 10. Time-varying amplitudes for SeaWiFS and SST combined EOF modes 1, 2, 3. Units are dimensionless and scaled for clarity.

functions are inversely related between color and temperature. While the spatial functions become noisier in the CZCS record at modes 2 and higher, the coincident SST spatial functions show patterns consistent with those during the SeaWiFS era (Fig. 11). Combining CZCS with SST has the advantage of enabling dominant spatial functions to be evident in the SST record because it had more complete coverage than CZCS.

For both SeaWiFS and CZCS eras, mode 1 is a seasonal signal and explains 42–43% of the variability as previously reported for EOFs on SST images (Everson et al. 1997). Even though the data have been temporally and spatially de-meaned, mode 1 shows that the MAB is out of phase with the GOM. The MAB shelf area has higher relative chlorophyll concentrations and lower temperatures during winter months (Nov–May), whereas in general, Georges Bank and the northeastern GOM are relatively cooler and have greater relative chlorophyll concentrations during summer (Jun–Oct). In the GOM, mode 1 SST during both the CZCS and SeaWiFS era differs from chlorophyll in that the southwestern GOM is out of phase with the northeastern GOM and Georges Bank.

Mode 2 explains 16–17% of the variability. CZCS and SeaWiFS chlorophyll spatial patterns are complex and differ somewhat from each other. For SeaWiFS, mode 2 shows high chlorophyll concentrations on Georges Bank and some areas of the MAB during spring and summer (Apr–Jul). Only

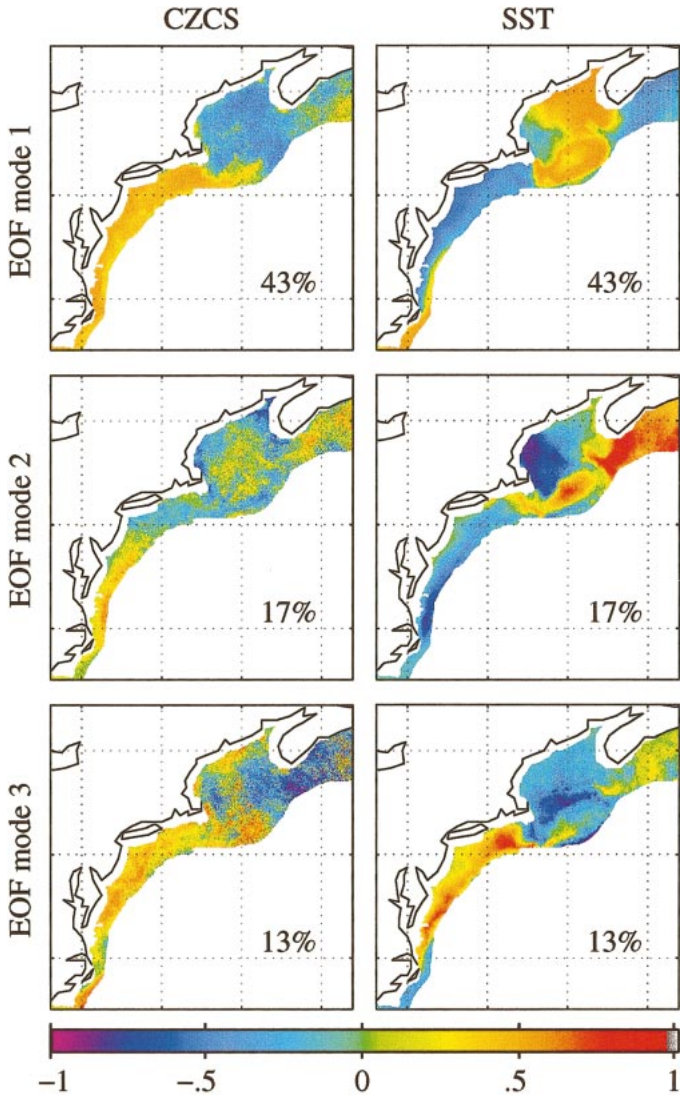


Fig. 11. Spatial eigenfunctions for CZCS and SST combined EOF modes 1, 2, 3. Units are dimensionless and scaled for clarity.

a hint of this pattern is evident in the mode 2 CZCS chlorophyll. For Georges Bank, SeaWiFS and CZCS mode 2 chlorophyll patterns are associated with colder SST during April–July. This relation is likely caused by the effects of strong tidal mixing, which keeps the bank destratified in summer, causing cooler temperatures and relatively high nutrient flux (Sathyendranath et al. 1991; Bisagni and Sano 1993). In the GOM, mode 2 SST and SeaWiFS chlorophyll EOFs are not as closely related as for mode 1 (Fig. 9). SeaWiFS chlorophyll spatial functions in the GOM show north–south differences, whereas SST EOFs show more of an east–west orientation. Combining the spatial pattern information with the amplitude time series (Fig. 10) shows that SST is relatively high during late spring and summer (May–Jul) in the western GOM compared to the eastern GOM, but the opposite pattern prevails in the fall (Sep–Dec). These differences are likely explained by differences in the salinity-induced stratification patterns between the western and eastern GOM. The western GOM is more stably stratified during

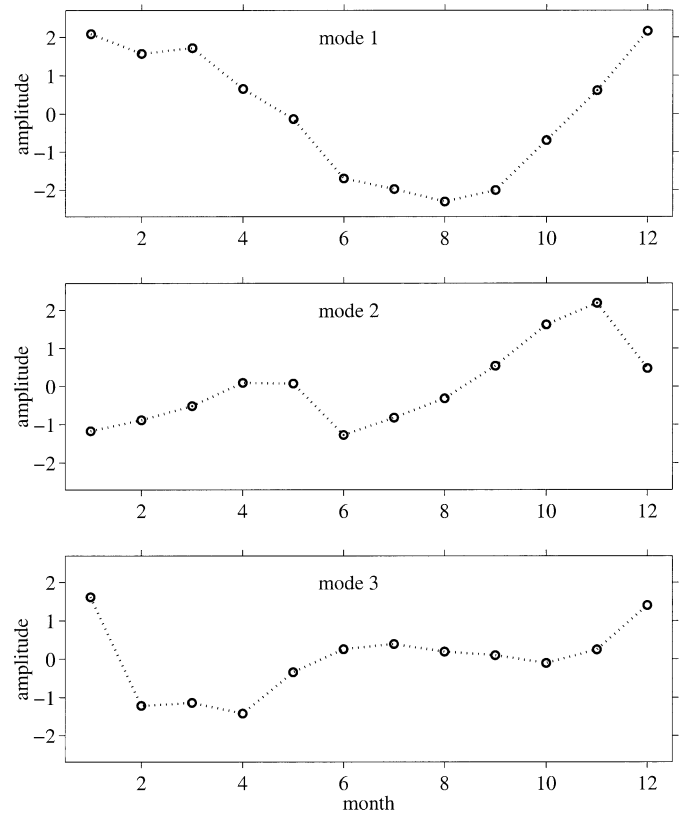


Fig. 12. Time-varying amplitudes for CZCS and SST combined EOF modes 1, 2, 3. Units are dimensionless and scaled for clarity.

summer but is well-mixed in fall and winter compared to the eastern GOM (Mountain and Manning 1994). Comparatively high SeaWiFS chlorophyll concentrations during fall in the western GOM are related to destratification and nutrient supply. A different water mass of Scotian shelf origin predominates in the eastern GOM (Mountain and Manning 1994; Yentsch et al. 1995), and the presence of this water mass of northern origin is the likely explanation for the common mode 2 SST and SeaWiFS chlorophyll pattern in the eastern GOM and Scotian shelf. Our SeaWiFS chlorophyll/SST mode 2 is very similar to mode 3 SST determined by others in a study focused specifically on Georges Bank and the GOM (Bisagni et al. 2001). Mode numbering will differ depending on the specific boundaries of the studies, as well as the data pretreatment; the spatial boundaries of our study covered a much larger area than Bisagni et al.'s (2001), and they did not de-mean twice and normalize prior to calculating EOFs as we did.

Finally, mode 3 explains 12–13% of the variability. For SeaWiFS and SST, mode 3 accentuates some key regional features of the seasonal cycle in MAB outer shelf and slope waters and in the western GOM. For these areas, the amplitude time series (Fig. 10) indicate that the spring increase (bloom) during April/May is the dominant component of this mode, although low concentrations in winter (Jan–Feb) and summer (Jul–Aug) also contribute. CZCS mode 3 is very different from SeaWiFS and not easily interpreted. However, the patterns evident in SeaWiFS mode 3, specifically the

spring bloom in MAB outer shelf waters, were also observed in EOF modes based on CZCS data that were averaged into 45-day bins over very large areas ($\sim 100 \text{ km}^2$) (Yoder et al. 2001).

The three chlorophyll climatologies (CZCS, SeaWiFS, and in situ) are very similar at mode 1, which explains about half of the variability seen off the coast of the U.S. Northeast after de-meaning and normalizing. The main feature of this mode is that the Gulf of Maine is out of phase with the mid-Atlantic Bight, with seasonally high chlorophyll concentrations in winter in the MAB and in summer in the GOM. CZCS diverges from the other two data sets at modes 2 and higher. It is not apparent from the chlorophyll comparisons alone whether this departure is caused by a real ecological difference between the two eras or some sensor or algorithm artifact. Pixel-to-pixel variability at modes 2 and 3 supports the latter interpretation. Although the SeaWiFS and in situ climatologies are correlated through mode 2, they diverge by mode 3. Lack of in situ data around Nova Scotia and south of Hatteras may account for some of the discrepancy in mode 3. Thus, all three data sets capture the dominant mean seasonal pattern (mode 0 in our terminology) and the most significant variation around this mean (mode 1). However, the three data sets represent other variations differently. The combined chlorophyll–temperature EOFs demonstrate consistent SST patterns between CZCS and SeaWiFS eras. Common eigenvalues, eigenfunctions, and time-varying amplitudes for both pairs are evidence that the dominant physical forcing was probably very similar during the two periods analyzed (1978–1986 and 1997–2000; note that AVHRR SST data were not available prior to 1985). Thus, the differences in satellite-derived chlorophyll concentrations between the mid-1980s and late 1990s are likely caused by as yet undescribed differences in nonphysical processes or artifacts in the CZCS data. The artifacts could be caused by having more missing data or less stable tuning and atmospheric correction than SeaWiFS. We lean toward the latter interpretation because our CZCS imagery was tuned with the in situ observations collected during the same era, yet SeaWiFS imagery shows better agreement with the three in situ modes than CZCS. Combined EOFs between SeaWiFS chlorophyll and SST elucidate interbasin differences in the GOM, possibly associated with the different water masses there. The co-EOFs also show that the spring (Apr–May) bloom in outer shelf waters of the MAB and in the western GOM accounts for just 12% of the variability. This is a correction to the mean seasonal pattern for these areas, and its effect is to increase the significance of the spring maximum in relation to fall. Our analyses also support earlier findings that the spring bloom in the central GOM is subordinate to the fall bloom (O'Reilly and Zetlin 1998).

References

- ANTOINE, D., AND A. MOREL. 1997. Atmospheric correction over the ocean (case I waters). MERIS Algorithm Theoretical Basis Document ATBD 2.7, December 5, 1997, p. 7-28–7-113.
- BAITH, K., G. FU, AND C. R. MCCLAIN. 2001. SeaDAS: Data analysis system developed for Ocean Color Satellite Sensors. EOS Trans. Am. Geophys. Union **82**: 202.
- BISAGNI, J. J., AND M. H. SANO. 1993. Satellite observations of sea surface temperature variability on southern Georges Bank. Cont. Shelf Res. **13**: 1045–1064.
- , K. W. SEEMANN, AND T. P. MAVOR. 2001. High-resolution satellite-derived sea-surface temperature variability over the Gulf of Maine and Georges Bank Region, 1993–1996. Deep-Sea Res. II **48**: 71–94.
- BRETHERTON, C. S., C. SMITH, AND J. M. WALLACE. 1992. An intercomparison of methods for finding coupled patterns in climate data. J. Clim. **5**: 541–560.
- BROWN, J. W., AND R. H. EVANS. 1993. Calibration of AVHRR infrared channels: A new approach to non-linear correction. J. Geophys. Res. **98**: 18,257.
- BROWN, O. B., R. H. EVANS, J. W. BROWN, H. R. GORDON, R. C. SMITH, AND K. S. BAKER. 1985. Phytoplankton blooming off the U.S. east coast: A satellite description. Science **229**: 163–167.
- CAMPBELL, J. W. 1995. The lognormal distribution as a model for bio-optical variability in the sea. J. Geophys. Res. **100**: 13,237–13,254.
- CAYULA, J.-F., AND P. CORNILLON. 1992. Edge detection algorithm for SST images. J. Atmos. Ocean. Technol. **9**: 67–80.
- CSANADY, G. T. 1990. Physical basis of coastal productivity. EOS **71**: 1060–1065.
- DAVIS, J. C. 1973. Statistics and data analysis in geology. Wiley.
- EMERY, W. J., AND R. E. THOMSON. 1998. Data analysis methods in physical oceanography. Elsevier.
- ESLINGER, D. L., J. J. O'BRIEN, AND R. L. IVERSON. 1989. Empirical orthogonal function analysis of cloud-containing Coastal Zone Color Scanner images of northeastern North American coastal waters. J. Geophys. Res. **94**: 10,884–10,890.
- EVANS, R. H. AND H. R. GORDON. 1994. Coastal zone color scanner “systems calibration.” A retrospective examination. J. Geophys. Res. **99**: 7293–7307.
- EVERSON, R., P. CORNILLON, L. SIROVICH, AND A. WEBBER. 1997. An empirical eigenfunction analysis of sea surface temperatures in the western North Atlantic. J. Phys. Oceanogr. **27**: 468–479.
- FLAGG, C. N., C. D. WIRICK, AND S. L. SMITH. 1994. The interaction of phytoplankton, zooplankton and currents from 15 months of continuous data in the mid-Atlantic Bight. Deep-Sea Res. II **41**: 411–436.
- FUENTES-YACO, C., A. F. VÉZINA, P. LAROCHE, C. VIGNEAU, M. GOSSELIN, AND M. LEVASSEUR. 1997. Phytoplankton pigment in the Gulf of St. Lawrence, Canada, as determined by the Coastal Zone Color Scanner—part I: Spatio-temporal variability. Cont. Shelf Res. **17**: 1421–1439.
- HOLM-HANSEN, O., C. J. LORENZEN, R. W. HOLMES, AND J. D. H. STRICKLAND. 1965. Fluorometric determination of chlorophyll. J. Cons. Perm. Int. Explor. Mer **30**: 3–15.
- KELLY, K. A. 1988. Comment on “Empirical orthogonal function analysis of advanced very high resolution radiometer surface temperature patterns in Santa Barbara channel” by G. S. E. Lagerloef and R. L. Bernstein. J. Geophys. Res. **93**: 15,753–15,754.
- LONGHURST, A. 1998. Ecological geography of the sea. Academic Press.
- LORENZ, E. N. 1956. Empirical orthogonal functions and statistical weather prediction. Statistical Forecasting Project, Department of Meteorology Science Report 1. Massachusetts Institute of Technology.
- MARRA, J., R. W. HOUGHTON, AND C. GARSIDE. 1990. Phytoplankton growth at the shelf-break front in the Middle Atlantic Bight. J. Mar. Res. **48**: 851–868.
- MCCLAIN, C. R., AND OTHERS. 2000. SeaWiFS postlaunch calibration and validation analyses, part 2. In S. B. Hooker and E. R.

- Firestone [eds.], NASA Technical Memo 2000-206892, V. 10, NASA Goddard Space Flight Center.
- MOUNTAIN, D. G., AND J. P. MANNING. 1994. Seasonal and inter-annual variability in the properties of the surface waters of the Gulf of Maine. *Cont. Shelf Res.* **14**: 1555–1581.
- NORTH, G. R., T. L. BELL, R. F. CAHALAN, AND F. J. MOENG. 1982. Sampling errors in the estimation of empirical orthogonal functions. *Mon. Weather Rev.* **110**: 699–706.
- O'REILLY, J. E., C. EVANS-ZETLIN, AND D. A. BUSCH. 1987. Primary production, p. 220–233. *In* R. H. Backus and D. W. Bourne [eds.], Georges Bank. MIT Press.
- , AND OTHERS. 1998. Ocean color chlorophyll algorithms for SeaWiFS. *J. Geophys. Res.* **103**: 24,937–24,953.
- , AND OTHERS. 2000. Ocean color chlorophyll *a* algorithms for SeaWiFS OC2 and OC4, Version 4. *In* S. B. Hooker and E. R. Firestone [eds.], SeaWiFS postlaunch calibration and validation analysis, Part 3. NASA Technical Memo 2000-206892, V. 11, NASA Goddard Space Flight Center.
- , AND C. ZETLIN. 1998. Seasonal, horizontal, and vertical distribution of phytoplankton chlorophyll *a* in the northeast U.S. continental shelf ecosystem. NOAA Technical Report NMFS 139. U.S. Department of Commerce.
- RYAN, J. P., J. A. YODER, AND P. C. CORNILLON. 1999. Enhanced chlorophyll at the shelfbreak of the mid-Atlantic Bight and Georges Bank during the spring transition. *Limnol. Oceanogr.* **44**: 1–11.
- , ———, AND D. W. TOWNSEND. 2001. Influence of a Gulf Stream warm-core ring on water mass and chlorophyll distributions along the southern flank of Georges Bank. *Deep-Sea Res II* **48**: 159–178.
- RYTHER, J. H., AND C. S. YENTSCH. 1958. Primary production of continental shelf waters off New York. *Limnol. Oceanogr.* **3**: 327–335.
- SATHYENDRANATH, S., T. PLATT, E. P. W. HORNE, W. G. HARRISON, O. ULLOA, R. OUTERBRIDGE, AND N. HOEPPFNER. 1991. Estimation of new production in the ocean by compound remote sensing. *Nature* **353**: 129–133.
- TOWNSEND, D., AND R. SPINRAD. 1986. Early spring phytoplankton blooms in the Gulf of Maine. *Cont. Shelf Res.* **6**: 515–529.
- ULLMAN, D. S., AND P. C. CORNILLON. 1999. Satellite-derived sea surface temperature fronts on the continental shelf off the northeast U.S. coast. *J. Geophys. Res.* **104**: 23,459–23,478.
- WALSH, J. J., D. A. DIETERLE, AND E. E. ESAIAS. 1987. Satellite detection of phytoplankton export from the mid-Atlantic Bight during the 1979 spring bloom. *Deep-Sea Res.* **34**: 675–703.
- , T. E. WHITLEDGE, F. W. BARVENIK, C. D. WIRICK, S. O. HOWE, W. E. ESAIAS, AND J. D. SCOTT. 1978. Wind events and food chain dynamics within the New York Bight. *Limnol. Oceanogr.* **23**: 659–683.
- YENTSCH, C. S., AND D. W. MENZEL. 1963. A method for the determination of phytoplankton chlorophyll and phaeophytin by fluorescence. *Deep-Sea Res.* **10**: 221–231.
- , J. W. CAMPBELL, AND S. APOLLONIO. 1995. A garden in the sea, p. 60–74. *In* P. W. Conkling [ed.], From Cape Cod to the Bay of Fundy: An environmental atlas of the Gulf of Maine. MIT Press.
- YODER, J. A., J. E. O'REILLY, A. H. BARNARD, T. S. MOORE, AND C. M. RUHSAM. 2001. Variability in Coastal Zone Color Scanner (CZCS) chlorophyll imagery of ocean margin waters off the U.S. east coast. *Cont. Shelf Res.* **21**: 1191–1218.

Received: 12 July 2001

Accepted: 18 December 2001

Amended: 7 January 2002